UMYU Scientifica, Vol. 4 NO. 3, September 2025, Pp 097 – 107
https://doi.org/10.56919/2543.010
ISSN: 2955 – 1145 (print); 2955 – 1153 (online)
A periodical of the Faculty of Natural and Applied Sciences, UMYU, Katsina

ORIGINAL RESEARCH ARTICLE

Spatial and Temporal Variations of Aerosol Optical Depth Distribution Over West African Sub - Region Using VIIRS Satellite Data

*Bello Sa'adu[1], Usman M. Gana[2]
[1]Department of Physics Umaru Musa Yaradua University Katsina, Nigeria
[2]Department of Physics, Bayero University Kano, Nigeria

ABSTRACT
West Africa has experienced rapid urbanization, economic growth, population increase, and industrialization, with no serious attention paid to aerosol emissions in the past decade. Thus, understanding the spatial and temporal variation of aerosol optical depth (AOD) is urgently needed to evaluate the effectiveness of aerosol control activities. Based on the Visible Infrared Imaging Radiometer Suite (VIIRS) satellite, AOD was retrieved over West Africa from 2012–2024. The monthly data were utilized for the analysis. The ground-based AOD from AERONET at a 550 nm wavelength was interpolated for inter-comparison with VIIRS satellite AOD data over the study period. Statistical parameters such as mean, maximum, minimum, and standard deviation were calculated. The results show that the monthly average mean AOD value in Nigeria ranges from 0.25–0.84, in Benin from 0.35–0.91, and in Niger from 0.24–0.84. The annual average AOD in Nigeria and Niger varied between 0.41–0.55, while in Benin it varied between 0.44–0.58. In terms of season, Nigeria has the highest mean AOD value in spring (0.66) and the lowest in winter (0.37), Niger has the highest mean AOD value in summer (0.74) and the lowest in winter (0.26), and Benin has the highest mean AOD value in spring (0.70) and the lowest in autumn (0.39). In addition, the AOD fluctuated greatly in 2015 and 2022 in Nigeria with the highest standard deviation (0.54 and 0.47), while the AOD fluctuated in 2016 and 2015 with the highest standard deviation (0.55 and 0.45) in Niger and Benin, respectively. These results provide a robust basis for assessing regional climate–aerosol interactions, and the validation of satellite observations with ground-based measurements shows good agreement.

ARTICLE HISTORY
Received April 29, 2025
Accepted September 05, 2025
Published September 30, 2025

KEYWORDS
AOD; VIIRs; AERONET; Spatial; Temporal

INTRODUCTION
Aerosols are solid and liquid particles suspended in air, with diameters of up to several micrometers, such as smoke, haze, dust, particulate matter, and liquid droplets (Payra et al., 2023; Choi et al., 2019). These particles are emitted from both natural and anthropogenic sources (Wang et al., 2017). Aerosol particles scatter and absorb sunlight, and the scattering of light from the Earth's surface affects the atmospheric radiation balance (Lang-Yona et al., 2010). These particles can persist in the atmosphere from days to weeks and can be transported from one region to another (Winker et al., 2013). The optical parameters of aerosols, such as Aerosol Optical Depth (AOD), Ångström Exponent (AE), and Single Scattering Albedo (SSA), indicate important characteristics of aerosols, including column-integrated aerosol load, particle size, and light-absorbing properties, which depend on their chemical composition. Specifically, SSA measures the ratio of the scattering coefficient to the total extinction coefficient (Xinyu et al., 2022). These parameters are also important factors in climate change analysis (Deng et al., 2012). AOD is a primary aerosol parameter representing the amount of aerosol loading in the atmosphere, while AE is generally used to estimate aerosol particle size. Aerosols are classified by particle size: coarse-mode aerosols with diameters greater than 1 μm are dominant when the AE value is smaller than 0.7, whereas a higher AE (>1.8) indicates the dominance of fine-mode aerosols with diameters smaller than 0.1 μm. An AE value between 0.7 and 1.8 is typical of the accumulation mode, where aerosol diameters vary between 0.1 and 1 μm (Kaufman et al., 1995).

Aerosol Optical Depth (AOD) is an important indicator and key parameter for understanding atmospheric physics and regional air quality by quantifying the aerosol load in the atmosphere (Bhatia et al., 2018; Filonchyk et al., 2018; Li et al., 2019), and it is generally derived and estimated using satellite observations. There are two main methods to measure AOD in the atmosphere: ground-based observations using sun photometer measurements and remote sensing inversion, which relies on sensor data from satellite platforms (Bello et al., 2025). Moreover,

Correspondence: Bello Sa'adu. Department of Physics, Faculty of Natural and Applied Sciences, Umaru Musa Yaradua University Katsina, Nigeria. ✉ bellosaadu5222@gmail.com.
How to cite: Sa'adu, B. & Gana, U. M. (2025). Spatial and Temporal Variations of Aerosol Optical Depth Distribution Over West African Sub-Region Using VIIRS Satellite Data. *UMYU Scientifica*, 4(3), 097–107. https://doi.org/10.56919/2543.010

aerosols increase the rate of mortality and morbidity and may lead to accidents on roads as they reduce visibility levels. At present, different ground-based monitoring networks have been established to provide AOD data worldwide, such as the AERosol RObotic NETwork (AERONET) (Holben et al., 1998), the Sun-Sky Radiometer Observation Network (SONET) (Ma et al., 2016), and the Sky Radiometer Network (SKYNET) (Pilahome et al., 2022). There are also many remote sensors that can monitor AOD, such as the Moderate Resolution Imaging Spectroradiometer (MODIS) (Pilahome et al., 2022), the Visible Infrared Imaging Radiometer Suite (VIIRS) (He et al., 2018), the Advanced Very High Resolution Radiometer (AVHRR) (Xue et al., 2017), and the Ozone Monitoring Instrument (OMI) (Stammes et al., 2002). Among them, MODIS, developed by NASA and carried on the Terra and Aqua satellites, is widely used for studying regional AOD due to its advantages, such as easy accessibility and excellent spatial and temporal resolution.

Ground-based observation networks such as the Aerosol Robotic Network (AERONET) provide accurate time-series AOD observations at different sites around the world (Estellé et al., 2012; Cesnulyte et al., 2014). However, due to the limited number of observation sites, it is difficult to produce AOD data that cover large geographical areas (Liu et al., 2016; Aklesso et al., 2018). Satellite-based observations, such as the Moderate Resolution Imaging Spectroradiometer (MODIS) aerosol optical depth (AOD) products, have recently proved useful in ensuring the spatiotemporal continuity of AOD observations (Liu et al., 2016; Nichol et al., 2016). The MODIS AOD products provide daily operational retrievals over land based on the Dark Target (DT) or Deep Blue (DB) algorithms (Ma et al., 2014; He et al., 2018). The DT algorithm was developed to retrieve AOD only over dark surfaces (e.g., water and dense vegetation), whereas the DB algorithm works over both dark and bright surfaces (e.g., arid, semi-arid, and urban areas) (Tao et al., 2015; Fan et al., 2017).

In this paper, we used Visible Infrared Imaging Radiometer Suite (VIIRS) satellite remote sensing data over a long time period, together with ground-based sun photometer observations from AERONET, to verify the accuracy of the VIIRS AOD product. The aims of the study were to investigate the spatial and temporal distribution of AOD over the West African sub-region (Benin, Niger, and Nigeria) during the 12-year period from 2012 to 2024, to discuss the monthly, seasonal, and annual differences, and to analyze the spatial patterns of AOD, aerosol types, and development trends in the region.

DATA AND METHODS

Study Area

The study area is located in West Africa, covering Nigeria, Niger, and Benin. The combined territory of the three countries spans approximately from latitudes 4°N to 23°N and longitudes 1°E to 17°E, representing a complete transitional zone from the humid coastal areas of the Gulf of Guinea to the semi-arid Saharan desert. The study area comprises the entirety of Nigeria (923,769 km²), Niger (1,267,000 km²), and Benin (112,622 km²), making it one of the most populous regions on the continent, with a resident population of over 270 million, as shown in Figure 1.

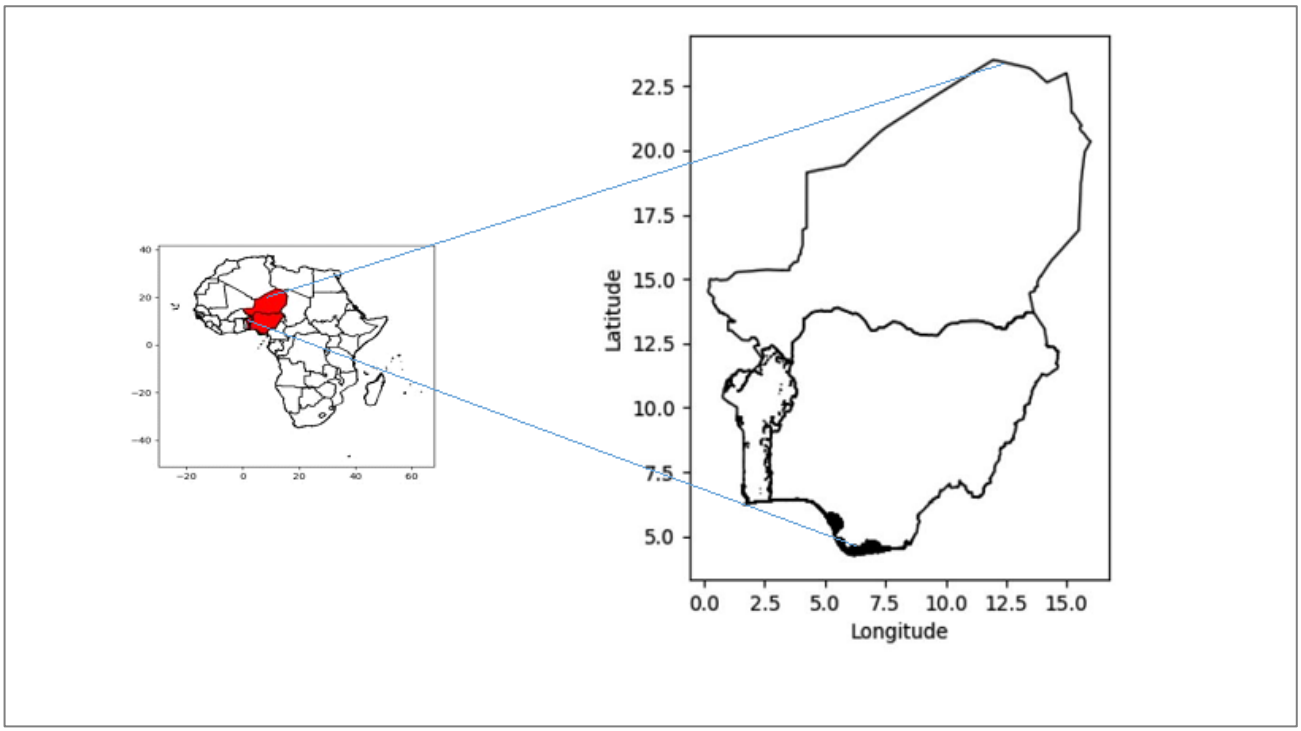

Figure 1: An over view map of the study area

Data

VIIRS Satellite

VIIRS is an instrument onboard the joint NASA and NOAA Suomi NPP mission (Zhou et al., 2016). It collects global observations across the visible and infrared wavelengths over the ocean, land, and atmosphere using a whiskbroom radiometer design. It was launched into space on 28 October 2011 into a sun-synchronous, polar orbit around the Earth (Xiong et al., 2013). The VIIRS sensor operates with a total of 22 spectral channels ranging from 0.412 µm to 12 µm (Moyer et al., 2018). The spatial resolution of VIIRS varies from 375 m to 750 m, and it covers the entire Earth twice daily (Oudrari et al., 2014). Suomi NPP crosses the equator at 1:30 a.m. (nighttime overpass) and 1:30 p.m. (daytime overpass) at the same local time (Payra et al., 2023).

AERONET

AERONET (Aerosol Robotic Network) is a global ground-based network that provides long-term measurements of aerosol optical properties at a wide range of wavelengths from 340 to 1640 nm with high temporal resolution. AERONET uses the CE-318 sun photometer to measure and provide data on aerosol optical, microphysical, and radiometric properties, and has been in operation for more than 25 years (Wang et al., 2023). It provides globally distributed observations of spectral aerosol optical depth (AOD), inversion products, and precipitable water across diverse aerosol regimes. Version 3 AOD data are computed for three data quality levels: Level 1.0 (unscreened data), Level 1.5 (cloud-screened and quality-controlled data), and Level 2.0 (cloud-screened and quality-assured data) (de Leeuw et al., 2018), corresponding to different sites.

Preprocessing of the Data

Preprocessing is the initial step in obtaining reliable AOD data for analysis. This cleaning process ensures consistency of the data and addresses potential issues. Daily AOD data were obtained from LAADS Web and aggregated into monthly, annual, and seasonal datasets. Missing values and outliers were discarded during preprocessing to ensure data integrity. AOD measurements that significantly deviated from the expected range of values in a dataset were considered outliers. Because AOD data have a fine resolution, they were aggregated to match the AERONET data by calculating the average AOD values in each grid cell. This step ensured that the spatial resolution of the AOD data aligned with that of AERONET, enabling accurate comparisons and analyses. The retrieved VIIRS AOD data were then averaged to present a comprehensive view of air quality across monthly, seasonal, and annual timescales using Python and Excel.

Validation Method

To validate the reliability of VIIRS data in the West African region, three stations—Ilorin (Nigeria), Banizoumbou (Niger), and Djougou (Benin)—were selected for validation. Based on the inversion of VIIRS, the AOD value at 550 nm was obtained. However, only two stations matched the timescale of the VIIRS satellite, as the Djougou site ceased operation in 2007, while VIIRS was launched in 2011. To compare and analyze the sun photometer data with VIIRS remote sensing AOD products, and to better match the AOD values of the products at the corresponding wavelength bands and spatial and temporal scales, the AOD value at 550 nm was obtained from the sun photometer data (AERONET) using the angstrom exponential formula. By applying AOD data at wavelengths close to 550 nm, typically 500 nm and 675 nm, the AOD at 550 nm was calculated for the sun photometer data (Zhu et al., 2023). According to Angstrom's formula:

$$\tau_{550} = \beta \times 500^{-\alpha} \quad (1)$$

$$\alpha = -\frac{ln\left(\frac{\tau_{500}}{\tau_{675}}\right)}{ln\frac{500}{675}} \quad (2)$$

$$\beta = \frac{\tau_{550}}{500^{-\alpha}} \quad (3)$$

where α is the Angstrom exponent(500-675nm), estimated from the slope of the spectral AOD plots in logarithmic scales, β is the turbidity coefficient, τ_{500}means AOD at 550 nm, and τ_{675}means AOD at 675 nm

$$x = \frac{1}{n}\sum_{i=1}^{n} x_i \quad (4)$$

$$\sigma = \sqrt{\frac{1}{n}\sum_{i=1}^{n}(x - \bar{x})^2} \quad (5)$$

Where $\bar{x}$ is the arithmetic mean of VIIR AOD, and x_i is the ith AOD sample value with n number of samples.

$$R = \frac{\sum_{i=1}^{n}(x_i - \bar{x})(y_i - \bar{y})}{\sqrt{\sum_{i}^{n}(x_i - \bar{x})^2 \times (y_i - \bar{y})^2}} \quad (6)$$

R is the correlation between the variable x and the variable y; $x_i$is the AOD for a year i; $y_i$is the value of another AOD variable in year i; x is the average AOD over the study period; y is the average of the other variables over the study period.

RESULTS AND DISCUSSION

Correlation of AOD Measurements

The VIIRS satellite AOD was compared with ground-based AOD observations over AERONET stations (Ilorin, Banizoumbou, and Djougou), as shown in Figures 3 and 4. Figures 3(a) and 4(c) demonstrate strong agreement between VIIRS and AERONET measurements, with correlation coefficients (R^2) of 0.91 for Nigeria and 0.81 for Niger, consistent with previous studies (Wang et al., 2023). Figures 3(c) and 4(d) further show that the highest VIIRS AOD occurred in 2016 and the lowest in 2012, while AERONET recorded its maximum in 2022 and minimum in 2024.

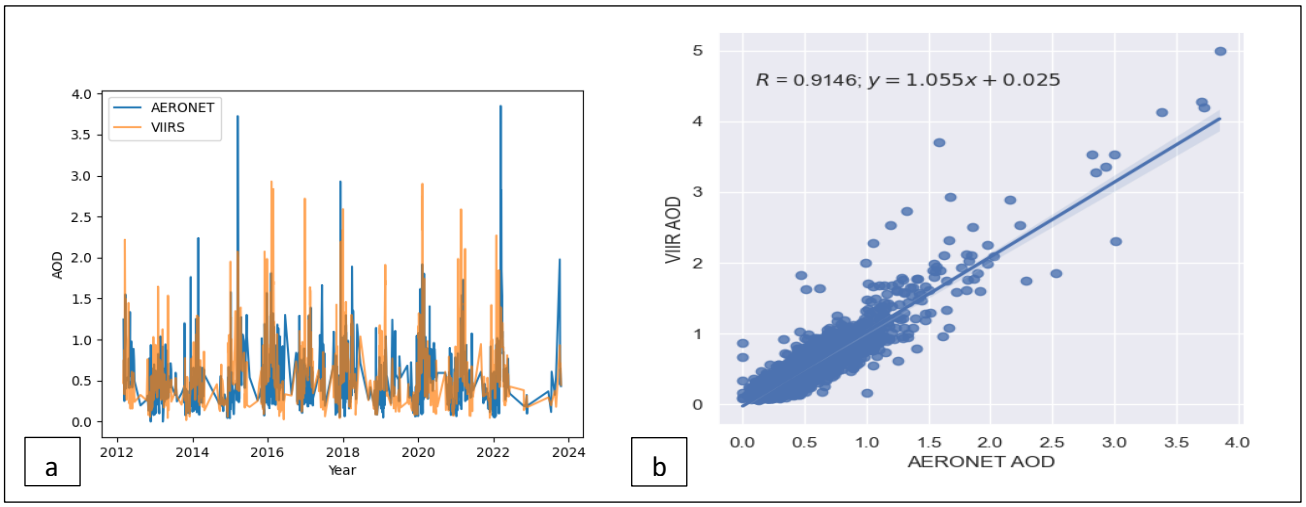

Figure 3: Comparison of VIIR data with AERONET data observations for Banizoumbou

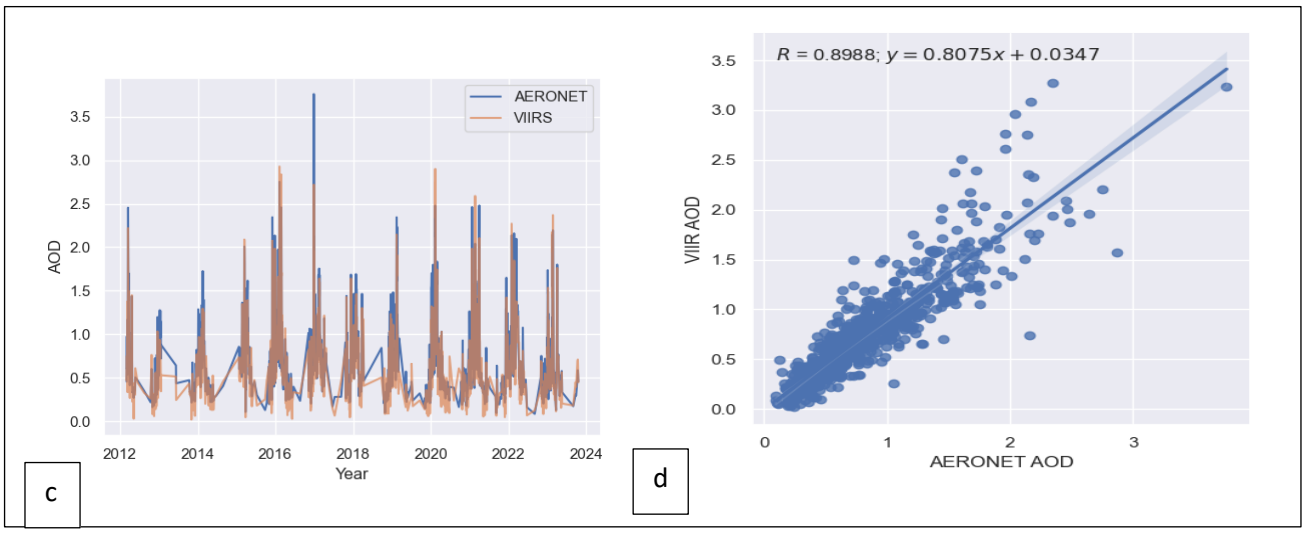

Figure 4: Comparison of VIIR data with AERONET data observations for Ilorin

Monthly mean AOD for Nigeria, Niger, and Benin over the last decade is presented in Figures 5, 6 and 7. AOD fluctuated seasonally, peaking in February for Nigeria and Benin, and in June for Niger. The monthly mean exceeded 0.8 in Nigeria and Benin, and 0.7 in Niger. These seasonal maxima are attributed to enhance Saharan dust transport and biomass burning, which increase aerosol loading during these months.

Figures 8, 9 and 10 show interannual variation of mean AOD and its standard deviation (STD) for 2012–2024. The highest AOD values were observed in 2015–2017 and 2022, when mean AOD exceeded 0.5 across the countries. These peaks reflect intense dust outbreaks and biomass burning episodes, whereas declines in other years correspond to reduced dust activity and more efficient aerosol removal by precipitation. The STD followed the same trend, with greater variability during years of high AOD, indicating more heterogeneous aerosol conditions. In contrast, years with lower AOD were characterized by smaller STD, suggesting more stable and less extreme aerosol concentrations.

Temporal Variations in AOD

The monthly minimum, maximum, mean, and standard deviation of AOD recorded in Nigeria, Niger, and Benin from 2012 to 2022 are summarized in Tables 1, 2, and 3. The annual mean AOD values were 0.49, 0.48, and 0.50,

with corresponding standard deviations of 0.43, 0.42, and 0.28, respectively, indicating moderate variability. The minimum AOD dropped as low as 0.0490 for Nigeria and Niger, and 0.0182 for Benin, while the maximum reached up to 5 across the countries. In terms of seasonal variability, January exhibited the lowest mean AOD (0.25 for Nigeria, 0.24 for Niger, and 0.34 for Benin), whereas June showed the highest mean AOD in Nigeria (0.84) and Niger (0.84), and February in Benin (0.94).

The higher mean AOD values observed in Niger are primarily driven by Sahelian and Bodélé Depression dust transport, reinforced by frequent storm events (Prospero et al., 2020; Ridley et al., 2014). In Benin, elevated mean AOD values occur during the dry-season months, particularly in February. This pattern reflects Benin's coastal location, where Harmattan dust transported from the north, combined with widespread regional biomass burning, dominates the aerosol regime (Jury & Santiago, 2010; Malavelle et al., 2011).

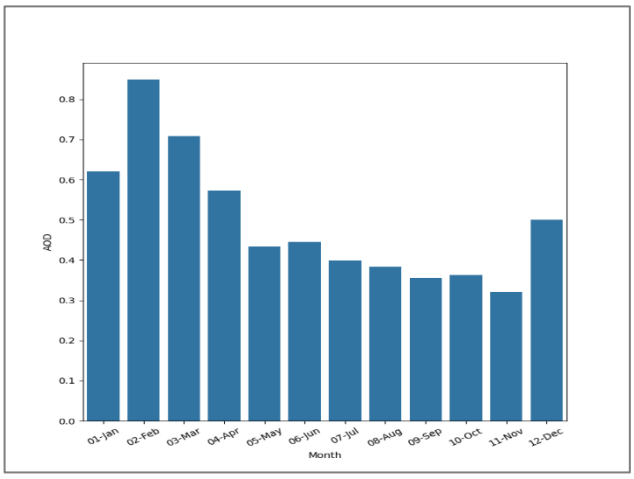

Figure 5: Variation of the monthly mean of AOD over Nigeria

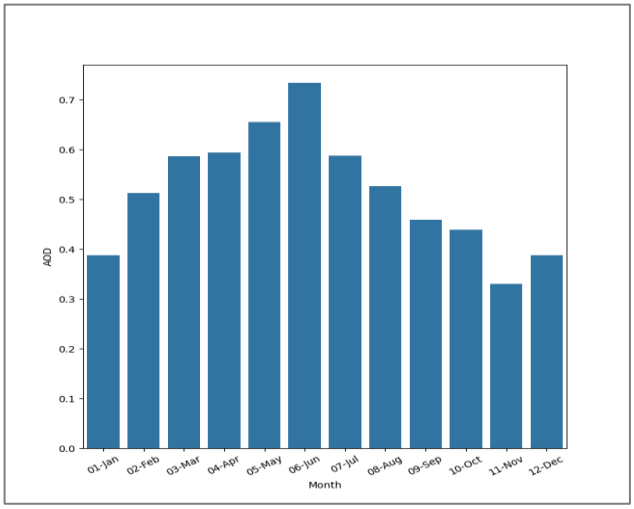

Figure 6: Variation of the monthly mean of AOD over Niger

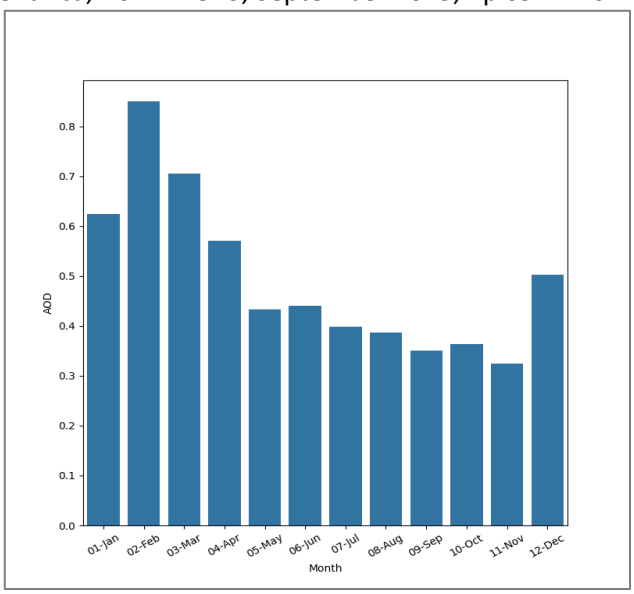

Figure 7: Variation of the monthly mean of AOD over Benin

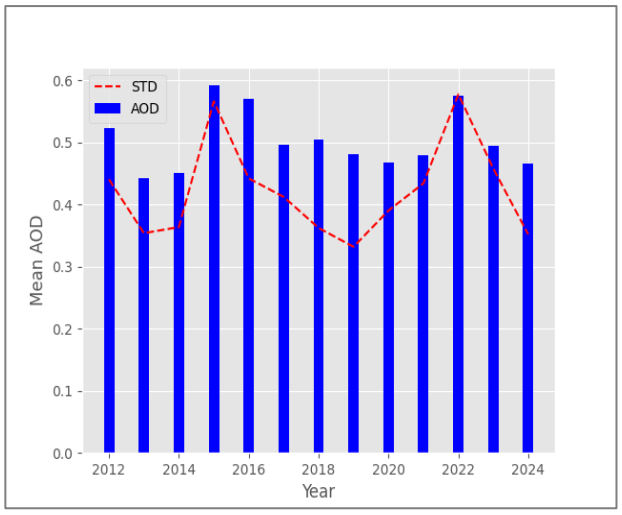

Figure 8: Variation of the annual mean of AOD Red curve indicate a standard deviation over Nigeria

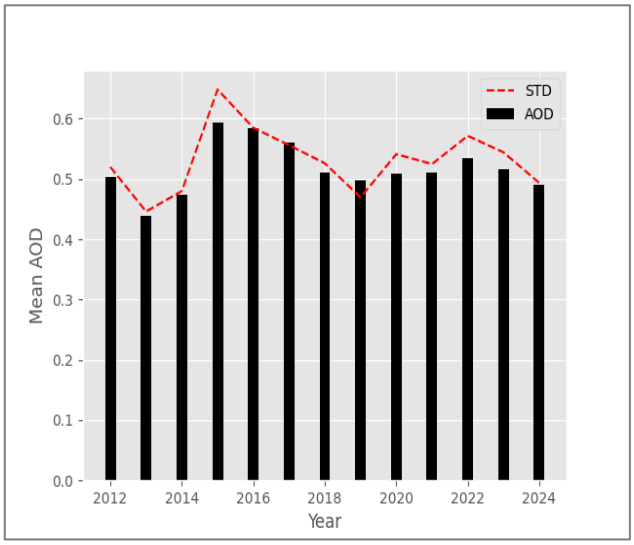

Figure 9: Variation of the annual mean of AOD Red curve indicate a standard deviation over Niger

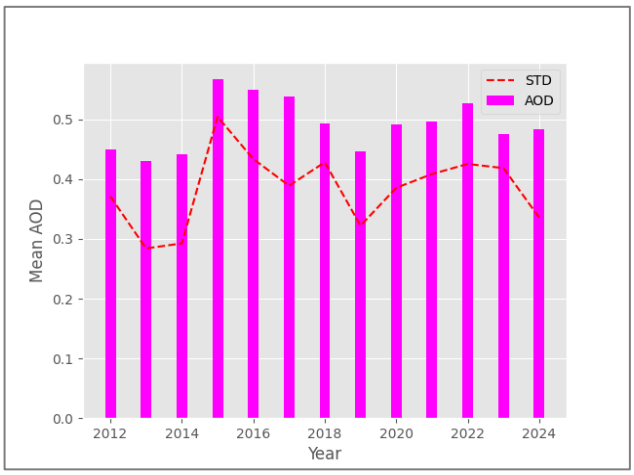

Figure 10: Variation of the annual mean of AOD over Benin

Seasonal and Inter-annual Variations in AOD

The analysis of seasonal AOD over Nigeria, Niger, and Benin (Table 4, 5 and 6) reveals distinct temporal variations that reflect the combined influence of dust transport, biomass burning, and rainfall seasonality. Niger shows pronounced variability consistent with regional climatic and emission dynamics. The highest mean AOD values for Nigeria and Benin are observed during spring (0.66; SD = 0.58 and 0.73; SD = 0.46, respectively), while Niger records its highest mean AOD during summer (0.73; SD = 0.62). In contrast, autumn (mean = 0.37; SD = 0.30) and winter (mean = 0.37; SD = 0.34) exhibit relatively lower AOD values. The spring maximum is particularly significant, corresponding to the onset of the West African biomass burning season in Nigeria and reflecting the combined influence of Saharan dust outbreaks and enhanced convective activity that uplift mineral particles into the atmosphere. In Niger, spring coincides with the peak dust season in the Sahel.

The spatial distribution of the average AOD across the study period is depicted in Figures 11, 12, and 13, revealing distinct patterns with concentrations of high AOD values exceeding 0.5, 1.5, and 0.6 in Nigeria, Niger, and Benin, respectively. Particularly hazy conditions were observed in January and February for Nigeria, and in July and August for Niger and Benin. Various factors, including increased anthropogenic activities and meteorological conditions such as low wind speeds, elevated air temperatures, and high humidity in the region, likely contributed to this spatial variability. The inter-annual spatial distribution further reveals significant variability from 2012 to 2024, with annual average AOD values fluctuating under the combined influence of natural and anthropogenic drivers. Consistently high AOD concentrations were recorded in 2024 and 2023 for Nigeria and Benin, whereas Niger showed relatively stable values throughout the study period. The seasonal spatial distributions of AOD, also presented in the figures, illustrate consistent patterns across the countries, with winter and autumn showing the highest average AOD values in Nigeria, summer and autumn in Niger, and spring and winter in Benin. Notably, winter exhibited high concentrations of coarse particles in Nigeria and spring in Benin, owing to increased Saharan dust transport over the area. The elevated AOD in winter is likely attributable to enhanced aerosol loading in the atmospheric column, particularly in the upper atmosphere, driven by long-range Saharan dust transport (Torabi et al., 2024).

Table1: Monthly observation of Nigeria from 2012-2024

Month	Observation	Minimum	Mean	Maximum	Std
January	31248	0.0495	0.2473	3.0018	0.2137
February	28476	0.0490	0.3465	4.9991	0.3505
March	33600	0.0493	0.4419	5.0000	0.4772
April	32676	0.0499	0.4819	4.9577	0.4411
May	33600	0.0546	0.6690	5.0000	0.5908
June	32760	0.0577	0.8437	5.0000	0.6981
July	33012	0.0563	0.7082	5.0000	0.5697
August	33096	0.0545	0.6597	5.0000	0.5463
September	32760	0.0555	0.4953	4.9940	0.3976
October	33684	0.0527	0.3983	5.0000	0.3628
November	31332	0.0523	0.2792	4.4334	0.2179
December	33684	0.0499	0.2784	4.7296	0.2527
Annual mean			0.4875		0.4265

Table 2: Monthly observation of Niger from 2012-2024

Month	Observation	minimum	Mean	maximum	Std
January	28145	0.0495	0.2430	3.0018	0.2107
February	26257	0.0490	0.3408	4.9991	0.3453
March	30933	0.0493	0.4349	5.0000	0.4687
April	30118	0.0499	0.4732	4.9578	0.4373
May	30917	0.0546	0.6501	5.0000	0.5613
June	31151	0.0577	0.8389	5.0000	0.6963
July	30752	0.0563	0.7078	5.0000	0.5707

To be continued next page

Table 2 continued

Month	Observation	minimum	Mean	maximum	Std
August	27806	0.0545	0.6698	5.0000	0.5616
September	29672	0.0555	0.4918	4.9940	0.4030
October	31999	0.0527	0.3920	5.0000	0.3541
November	28829	0.0523	0.2752	4.4334	0.2172
December	30608	0.0499	0.2727	4.7296	0.2468
Annual mean			0.4825		0.4228

Table 3: Monthly observation of Benin from 2012-2024

Month	Observation	Minimum	Mean	Maximum	Std
January	13117	0.0906	0.7203	4.8724	0.3211
February	10575	0.1551	0.9411	4.0145	0.4351
March	9190	0.0293	0.6512	5.0000	0.4564
April	7628	0.0275	0.5223	5.0000	0.3634
May	6759	0.0200	0.3675	3.6078	0.2016
June	4482	0.0267	0.3769	5.0000	0.2439
July	2577	0.0242	0.3825	4.9991	0.1805
August	2350	0.0288	0.4109	1.5634	0.1684
September	3563	0.0284	0.3446	1.8979	0.1965
October	7210	0.0325	0.3781	4.3341	0.2682
November	11004	0.0182	0.3580	1.7617	0.1730
December	14377	0.0246	0.5621	4.4186	0.3585
Annual mean			0.5013		0.2806

Table 4: Seasonal statistic of average AOD for Nigeria during 2012-2024

Season	Observation	Minimum	Mean	Maximum	Std
Autumn	1607	0.0545	0.3710	3.0196	0.2977
Spring	2017	0.0714	0.6556	4.9885	0.5795
Summer	1790	0.0746	0.6230	3.1204	0.4019
Winter	2105	0.0545	0.3674	4.9514	0.3383

Table 5: Seasonal statistic of average AOD for Niger during 2012-2024

Season	Observation	Minimum	Mean	Maximum	Std
Autumn	89477	0.0527	0.5114	5.0000	0.4580
Spring	87308	0.0490	0.4198	5.0000	0.4273
Summer	92820	0.0546	0.7326	5.0000	0.6179
Winter	87582	0.0495	0.2640	4.7296	0.2265

Table 6: Seasonal statistic of average AOD for Benin during 2012 -2024

Season	Observation	Minimum	Mean	Maximum	Std
Autumn	13123	0.028437	0.374862	4.334073	0.235738
Spring	27393	0.027503	0.727219	5	0.459396
Summer	13818	0.020035	0.37338	5	0.212805
Winter	38498	0.018177	0.557645	4.872363	0.334826

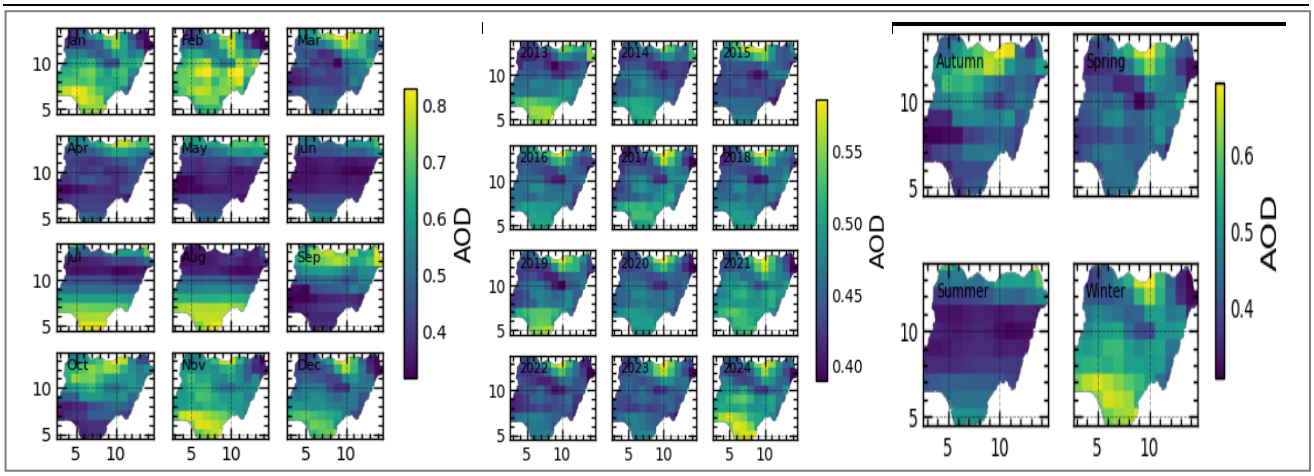

Figure 11: Spatial distribution of AOD from 2012 to 2024 over Nigeria

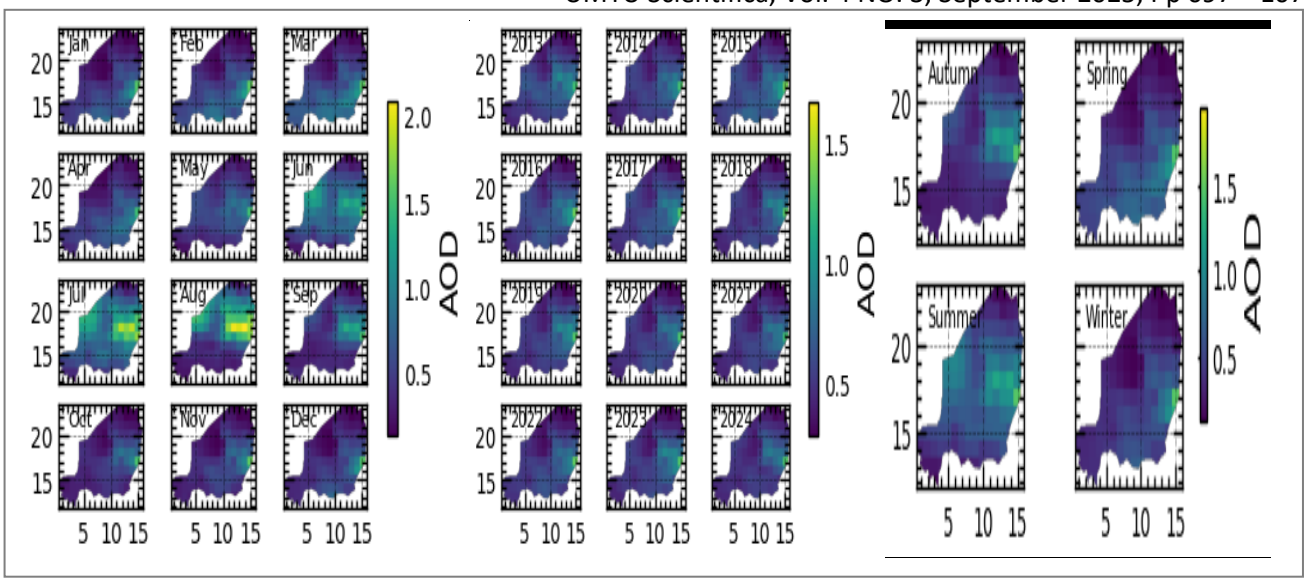

Figure 12: Spatial distribution of AOD from 2012 to 2024 over Niger

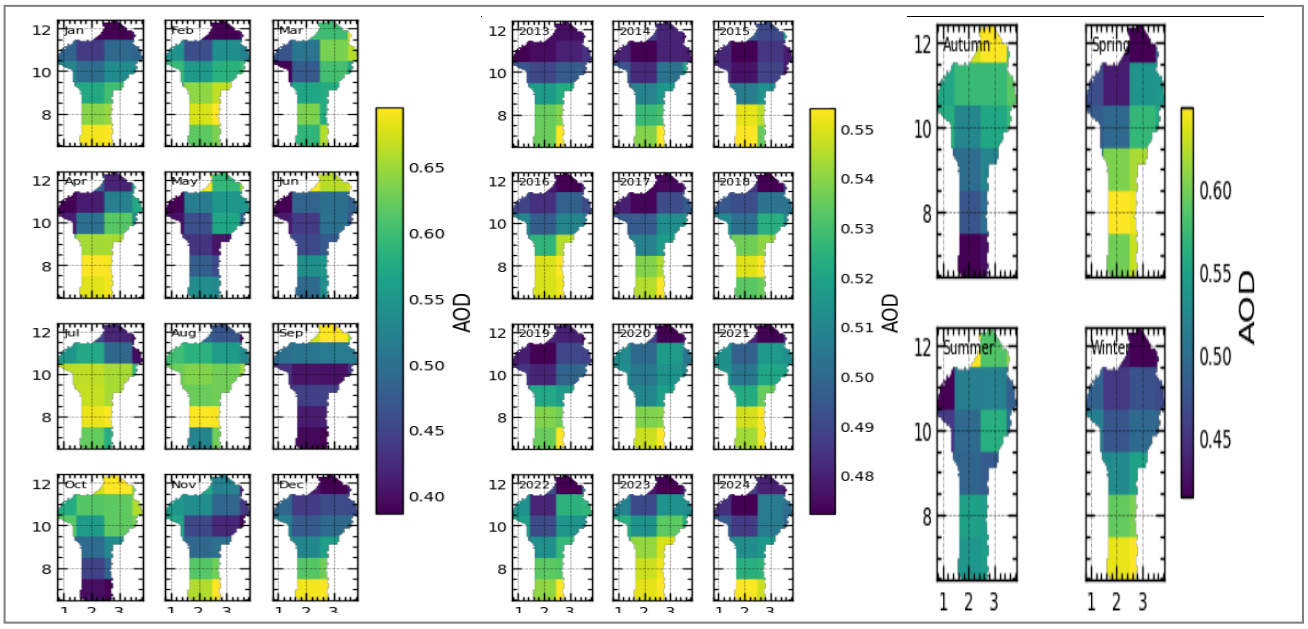

Figure 13: Spatial distribution of AOD from 2012 to 2024 over Benin

Aerosol Classification

The Angstrom Exponent (AE), derived from AERONET, is used to characterize aerosol size and types, as shown in Figures 14, 15 and 16 for the VIIRS satellite data (a–c) over the three regions. AE exploits the different responses of two wavelengths to aerosol loading and characterizes the size of aerosol particles. This parameter is particularly useful for distinguishing between fine aerosols (biomass burning, BB; vehicular emissions, VE), coarse aerosols (desert dust, DD; sea salt, SS), and mixed aerosols (BB/DD and VE/SS) for the purpose of identifying aerosol clusters. When AOD concentrations are low, there is a non-negligible uncertainty in the calculated AE; therefore, AE parameters are compared only when the AERONET 550 nm AOD is greater than 0.2 (Li et al., 2022). Figures 14, 15 and 16 indicate that desert dust (DD) and sea salt (SS) are dominant in the region (AE < 1), reflecting the prevalence of coarse particles. This is consistent with the geographical setting of the study area, which is strongly influenced by long-range Saharan dust transport and marine aerosols from the Atlantic Ocean. In particular, Niger shows persistent dust dominance linked to the Bodélé Depression, one of the world's most active dust sources, while coastal Benin reflects both desert dust intrusions and contributions from marine aerosols. Nigeria, located in the transitional zone, shows signatures of both dust outbreaks and local fine aerosols.

A moderate level of mixed particles (BB/DD) is also evident in the region (cyan clusters), especially during the dry season, when biomass burning emissions coincide with dust outbreaks. This mixture highlights the complexity of aerosol sources in West Africa, where natural processes such as dust uplift interact with anthropogenic activities such as agricultural residue burning, traffic emissions, and industrial activities. The dominance of coarse particles underscores their major role in modulating regional radiative forcing, visibility

reduction, and health impacts, while the seasonal variability of mixed aerosols indicates a dynamic interplay between human-driven and natural aerosol sources.

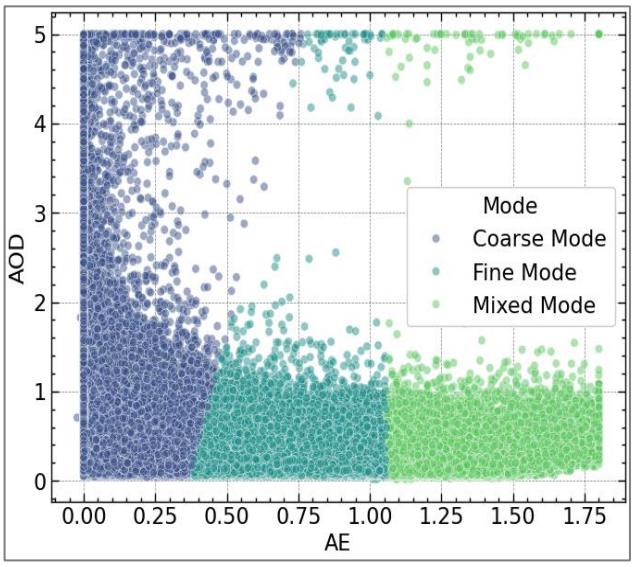

Figure 14: Plot of AOD against AE to Characterized the aerosol mode over Nigeria

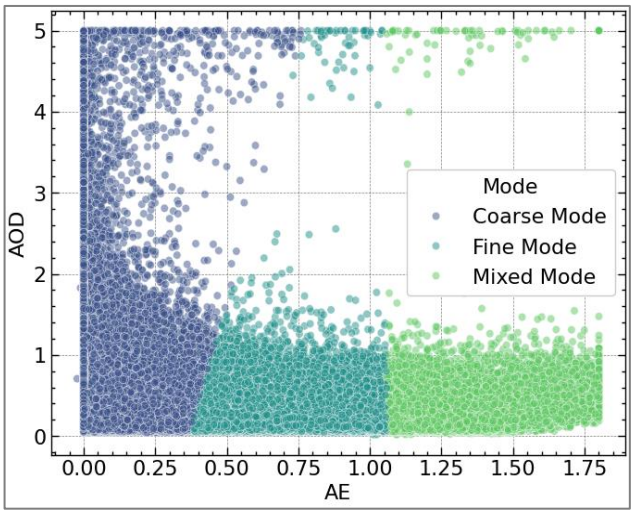

Figure 15: Plot of AOD against AE to Characterized the aerosol mode over Niger

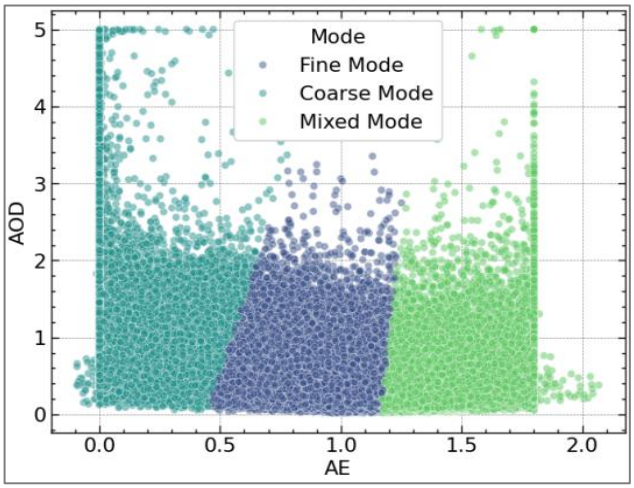

Figure 16: Plot of AOD against AE to Characterized the aerosol mode over Benin

CONCLUSIONS

This study reveals that aerosol optical depth (AOD) over West Africa exhibits marked spatial and temporal variability, shaped by biomass burning, Saharan dust transport, and meteorological factors. The results show that Nigeria and Niger record their highest AOD values in spring and summer, while Benin peaks in spring due to the combined influence of dust and biomass burning. Seasonal cycles consistently highlight a summer maximum and winter minimum, in agreement with Saharan dust climatology, while interannual variations were most pronounced in 2015, 2016, and 2022. The correlation between VIIRS and AERONET data demonstrates strong consistency (R^2 = 0.91 and 0.81 for Nigeria and Niger), confirming the reliability of satellite observations. Analysis of aerosol modes indicates that Niger is strongly dust-dominated, Benin is influenced by biomass burning and rainfall, and Nigeria represents a transitional zone between Sahelian and coastal climates. These findings not only improve understanding of aerosol sources and transport mechanisms in the sub-region but also have important implications for air quality monitoring, climate modeling, and policymaking aimed at mitigating the impacts of atmospheric aerosols on health and the environment.

REFERENCES

Adesina, A. J., Kumar, K. R., Sivakumar, V., & Piketh, S. (2016). Inter-comparison and assessment of long-term (2003-2013) multiple satellite aerosol products over two contrasting sites in South Africa. *Atmospheric Environment, 125*, 494–506. [Crossref]

Aklesso, M., Kumar, K. R., Bu, L., & Boiyo, R. (2018). Analysis of spatial-temporal heterogeneity in remotely sensed aerosol properties observed during 2005-2015 and SKYRAD4.2 inversion products retrieved from a Cimel CE318 sun photometer. *Atmospheric Measurement Techniques, 11*(11), 6049–6064. [Crossref]

Bello, B. I., Tijjani, B. S., & Gana, U. M. (2025). Spatiotemporal variability of aerosol optical depth over Nigeria based on MODIS satellite observations (2004-2023). *Asian Journal of Research and Reviews in Physics, 9*(2), 47–59. [Crossref]

Bhatia, N., Tolpekin, V. A., Stein, A., & Reusen, I. (2018). Estimation of AOD under uncertainty: An approach for hyperspectral airborne data. *Remote Sensing, 10*(6), 947. [Crossref]

Cesnulyte, V., Lindfors, A. V., Pitkänen, M. R. A., Lehtinen, K. E. J., Morcrette, J.-J., & Arola, A. (2014). Comparing ECMWF AOD with AERONET observations at visible and UV wavelengths. *Atmospheric Chemistry and Physics, 14*(1), 593–608. [Crossref]

Choi, M., Lim, H., Kim, J., Lee, S., Eck, T. F., Holben, B. N., Garay, M. J., Hyer, E. J., Saide, P. E., & Liu, H. (2019). Validation, comparison, and integration of GOCI, AHI, MODIS, MISR, and

VIIRS aerosol optical depth over East Asia during the 2016 KORUS-AQ campaign. *Atmospheric Measurement Techniques, 12*(8), 4619–4641. [Crossref]

de Leeuw, G., Sogacheva, L., Rodriguez, E., Kourtidis, K., Georgoulias, A. K., Alexandri, G., Amiridis, V., Proestakis, E., Marinou, E., Xue, Y., & van der A, R. J. (2018). Two decades of satellite observations of AOD over mainland China using ATSR-2, AATSR and MODIS/Terra: Data set evaluation and large-scale patterns. *Atmospheric Chemistry and Physics, 18*(3), 1573–1592. [Crossref]

Deng, X., Shi, C., Wu, B., Chen, Z., Nie, S., He, D., & Zhang, H. (2012). Analysis of aerosol characteristics and their relationships with meteorological parameters over Anhui province in China. *Atmospheric Research, 109–110*, 52–63. [Crossref]

Estellés, V., Campanelli, M., Utrillas, M. P., Expósito, F., & Martínez-Lozano, J. A. (2012). Comparison of AERONET and SKYRAD4.2 inversion products retrieved from a Cimel CE318 sunphotometer. *Atmospheric Measurement Techniques, 5*(3), 569–579. [Crossref]

Fan, A., Chen, W., Liang, L., Sun, W., Lin, Y., Che, H., & Zhao, X. (2017). Evaluation and comparison of long-term MODIS C5.1 and C6 products against AERONET observations over China. *Remote Sensing, 9*(12), 1269. [Crossref]

Filonchyk, M., Yan, H., Zhang, Z., Yang, S., Li, W., & Li, Y. (2019). Combined use of satellite and surface observations to study aerosol optical depth in different regions of China. *Scientific Reports, 9*, 18650. [Crossref]

Ginoux, P., Prospero, J. M., Gill, T. E., Hsu, N. C., & Zhao, M. (2012). Global-scale attribution of anthropogenic and natural dust sources and their emission rates based on MODIS Deep Blue aerosol products. *Reviews of Geophysics, 50*(3). [Crossref]

He, L., Wang, L., Lin, A., Zhang, M., Bilal, M., & Wei, J. (2018). Performance of the NPP-VIIRS and aqua-MODIS aerosol optical depth products over the yangtze river basin. *Remote Sensing, 10*(1), 117. [Crossref]

He, Q., & Huang, B. (2018). Satellite-based mapping of daily high-resolution ground PM2.5 in China via space-time regression modeling. *Remote Sensing of Environment, 206*, 72–83. [Crossref]

Holben, B. N., Eck, T. F., Slutsker, I., Tanré, D., Buis, J. P., Setzer, A., Vermote, E., Reagan, J. A., Kaufman, Y. J., Nakajima, T., Lavenu, F., Jankowiak, I., & Smirnov, A. (1998). AERONET—A federated instrument network and data archive for aerosol characterization. *Remote Sensing of Environment, 66*(1), 1–16. [Crossref]

Jury, M. R., & Santiago, M. J. (2010). Atmospheric transport pathways to southern Africa and South America. *International Journal of Climatology, 30*(11), 1508–1522. [Crossref]

Kaufman, Y. J. (1995). Remote sensing of direct and indirect aerosol forcing. In R. J. Charlson & J. Heintzenberg (Eds.), *Aerosol forcing of climate* (pp. 297–332). John Wiley & Sons.

Kumar, K. R., Sivakumar, V., & Reddy, R. R. (2018). Multi-year climatological trends of aerosol optical properties over West Africa inferred from ground-based AERONET and satellite observations. *Atmospheric Research, 214*, 142–156. [Crossref]

Lang-Yona, N., Abo-Riziq, A., Erlick, C., Segre, E., Trainic, M., & Rudich, Y. (2010). Interaction of internally mixed aerosols with light. *Physical Chemistry Chemical Physics, 12*(1), 21–31. [Crossref]

Li, W., Su, X., Feng, L., Wu, J., Zhang, Y., & Cao, M. (2022). Comprehensive validation and comparison of three VIIRS aerosol products over the ocean on a global scale. *Remote Sensing, 14*(11), 2544. [Crossref]

Liu, X., Chen, Q., Che, H., Zhang, R., Gui, K., Zhang, H., & Zhao, T. (2016). Spatial distribution and temporal variation of aerosol optical depth in the Sichuan basin, China, the recent ten years. *Atmospheric Environment, 147*, 434–445. [Crossref]

Ma, Y., Li, Z., Li, Z., Xie, Y., Fu, Q., Li, D., Zhang, Y., Xu, H., & Li, K. (2016). Validation of MODIS aerosol optical depth retrieval over mountains in central China based on a sun-sky radiometer site of SONET. *Remote Sensing, 8*(2), 111. [Crossref]

Ma, Z., Hu, X., Huang, L., Bi, J., & Liu, Y. (2014). Estimating ground-level PM2.5 in China using satellite remote sensing. *Environmental Science & Technology, 48*(13), 7436–7444. [Crossref]

Malavelle, F. F., Pont, V., Mallet, M., & Tanré, D. (2011). Simulation of aerosol radiative effects over West Africa during DABEX and AMMA SOP-0. *Atmospheric Chemistry and Physics, 11*(6), 5769–5795. [Crossref]

Moyer, D., Moeller, C., & De Luccia, F. (2018). NOAA-20 VIIRS thermal emissive band calibration error comparison with heritage VIIRS sensors. In *Sensors, systems, and next-generation satellites XXII* (Vol. 10785, p. 107851U). International Society for Optics and Photonics. [Crossref]

N'Datchoh, E. T., Konaré, A., Diedhiou, A., Diawara, A., Quansah, E., & Assamoi, P. (2018). Effects of climate variability on savannah fire regimes in West Africa. *Earth System Dynamics, 9*(2), 663–681. [Crossref]

Nichol, J., & Bilal, M. (2016). Validation of MODIS 3 km resolution aerosol optical depth retrievals over Asia. *Remote Sensing, 8*(4), 328. [Crossref]

Oudrari, H., McIntire, J., Xiong, X., Butler, J., Lee, S., Lei, N., Schwarting, T., & Sun, J. (2014). Prelaunch radiometric characterization and calibration of the S-NPP VIIRS sensor. *IEEE Transactions on Geoscience and Remote Sensing, 53*(4), 2195–2210. [Crossref]

Payra, S., Sharma, A., Mishra, M. K., & Verma, S. (2023). Performance evaluation of MODIS and VIIRS satellite AOD products over the Indian

subcontinent. *Frontiers in Environmental Science, 11*. [Crossref]

Pilahome, O., Ninssawan, W., Jankondee, Y., Janjai, S., & Kumharn, W. (2022). Long-term variations and comparison of aerosol optical properties based on MODIS and ground-based data in Thailand. *Atmospheric Environment, 286*, 119218. [Crossref]

Prospero, J. M., Barkley, A. E., Gaston, C. J., Gatineau, A., Campos y Sansano, A., & Panechou, K. (2020). The atmospheric transport and deposition of mineral dust to the ocean: Implications for research needs. *Proceedings of the National Academy of Sciences, 117*(26), 14645–14654. [Crossref]

Ridley, D. A., Heald, C. L., & Ford, B. (2014). North African dust export and deposition: A satellite and model perspective. *Journal of Geophysical Research: Atmospheres, 119*(10), 6259–6277. [Crossref]

Stammes, P. (Ed.). (2002). *OMI algorithm theoretical basis document: Volume III: Clouds, aerosols, and surface UV irradiance* (2nd ed.). NASA Goddard Space Flight Center.

Tao, M., Chen, L., Wang, Z., Tao, J., Che, H., Wang, X., & Wang, Y. (2015). Comparison and evaluation of the MODIS Collection 6 aerosol data in China. *Journal of Geophysical Research: Atmospheres, 120*(14), 6992–7005. [Crossref]

Torabi, S. E., Amin, M., Phairuang, W., Lee, H.-M., Hata, M., & Furuuchi, M. (2024). High-resolution characterization of aerosol optical depth and its correlation with meteorological factors in Afghanistan. *Atmosphere, 15*(7), 849. [Crossref]

Wang, W., Mao, F., Pan, Z., Du, L., & Gong, W. (2017). Validation of VIIRS AOD through a comparison with a sun photometer and MODIS AODs over wuhan. *Remote Sensing, 9*(5), 403. [Crossref]

Wang, Y., Yang, L., Xie, D., Hu, Y., Cao, D., Huang, H., & Zhao, D. (2023). Investigation of spatiotemporal variation and drivers of aerosol optical depth in China from 2010 to 2020. *Atmosphere, 14*(3), 477. [Crossref]

Winker, D. M., Tackett, J. L., Getzewich, B. J., Liu, Z., Vaughan, M. A., & Rogers, R. R. (2013). The global 3-D distribution of tropospheric aerosols as characterized by CALIOP. *Atmospheric Chemistry and Physics, 13*(6), 3345–3361. [Crossref]

XinYu, X., Nichol, J. E., Lee, K. H., Li, J., & Wong, M. S. (2022). Analysis of long-term aerosol optical properties combining AERONET sunphotometer and satellite-based observations in Hong Kong. *Remote Sensing, 14*(20), 5220. [Crossref]

Xiong, X., Oudrari, H., Chiang, K., McIntire, J., Fulbright, J., Lei, N., & Wang, Z. (2013). VIIRS on-orbit calibration activities and performance. *2013 IEEE International Geoscience and Remote Sensing Symposium - IGARSS*, 520–523. [Crossref]

Xue, Y., He, X., de Leeuw, G., Mei, L., Che, Y., Rippin, W., & Hu, Y. (2017). Long-time series aerosol optical depth retrieval from AVHRR data over land in North China and Central Europe. *Remote Sensing of Environment, 198*, 471–489. [Crossref]

Yu, X., Nichol, J., Lee, K. H., Li, J., & Wong, M. S. (2022). Analysis of long-term aerosol optical properties combining AERONET sunphotometer and satellite-based observations in Hong Kong. *Remote Sensing, 14*(20), 5220. [Crossref]

Zhou, L., Divakarla, M., & Liu, X. (2016). An overview of the Joint Polar Satellite System (JPSS) science data product calibration and validation. *Remote Sensing, 8*(2), 139. [Crossref]

Zhu, Z., Zhang, Z., Liu, F., Chen, Z., Ren, Y., & Guo, Q. (2023). Study on accuracy evaluation of MCD19A2 and spatiotemporal distribution of AOD in arid zones of Central Asia. *Sustainability, 15*(18), 13959. [Crossref]